

1 **Long-term Trends in Aerosol and Precipitation Composition over the**
2 **Western North Atlantic Ocean at Bermuda (ACP-2014-131-Revised)**

3
4 William C. Keene^{1*}, Jennie L. Moody¹, James N. Galloway¹, Joseph M. Prospero²,
5 Owen R. Cooper³, Sabine Eckhardt⁴, and John R. Maben¹

6
7 ¹Department of Environmental Sciences, Clark Hall, University of Virginia, Charlottesville, VA,
8 22904-4123, USA

9 ²Division of Marine and Atmospheric Chemistry, University of Miami, 4600 Rickenbacker
10 Causeway, Miami, FL, 33149-1098, USA

11 ³Cooperative Institute for Research in Environmental Sciences (CIRES), University of Colorado
12 and NOAA Earth Systems Research Laboratory, Boulder, CO, 80305, USA

13 ⁴Norwegian Institute for Air Research, Kjeller, Norway

14 *Corresponding author (e-mail: wck@virginia.edu)

15

16

17 Abstract

18

19 Since the 1980s, emissions of SO_2 and NO_x ($\text{NO} + \text{NO}_2$) from anthropogenic sources in the
20 United States (US), Canada, and Europe have decreased significantly suggesting that the export
21 of oxidized S and N compounds from surrounding continents to the atmosphere overlying North
22 Atlantic Ocean (NAO) has also decreased. The chemical compositions of aerosols and
23 precipitation sampled daily on Bermuda (32.27 N, 64.87 W) from 1989 to 1997 and from 2006
24 to 2009 were evaluated to quantify the magnitudes, significance, and implications of associated
25 trends in atmospheric composition. The chemical data were stratified based on FLEXPART
26 retroplumes into four discrete transport regimes: Westerly flow from the eastern North America
27 (NEUS/SEUS); easterly trade-wind flow from northern Africa and the subtropical NAO (Africa);
28 long, open-ocean, anticyclonic flow around the Bermuda High (Oceanic); and transitional flow
29 from the relatively clean open ocean to the polluted eastern North America (North). Based on all
30 data, annual average concentrations of non-sea-salt (nss) SO_4^{2-} associated with aerosols and
31 annual volume-weighted-average (VWA) concentrations in precipitation decreased significantly
32 (by 22% and 49%, respectively) whereas annual VWA concentrations of NH_4^+ in precipitation
33 increased significantly (by 70%). Corresponding trends in aerosol and precipitation NO_3^- and of
34 aerosol NH_4^+ were insignificant. Nss SO_4^{2-} in precipitation under NEUS/SEUS and Oceanic
35 flow decreased significantly (61% each) whereas corresponding trends in particulate nss SO_4^{2-}
36 under both flow regimes were insignificant. Trends in precipitation composition were driven in
37 part by decreasing emissions of SO_2 over upwind continents and associated decreases in
38 anthropogenic contributions to nss SO_4^{2-} concentrations. Under NEUS/SEUS and Oceanic flow,
39 the ratio of anthropogenic to biogenic contributions to nss SO_4^{2-} in the column scavenged by
40 precipitation were relatively greater than those in near surface aerosol, which implies that, for
41 these flow regimes, precipitation is a better indicator of overall anthropogenic impacts on the
42 lower troposphere. Particulate nss SO_4^{2-} under African flow also decreased significantly (34%)
43 whereas the corresponding decrease in nss SO_4^{2-} associated with precipitation was insignificant.
44 We infer that these trends were driven in part by reductions in the emissions and transport of
45 oxidized S compounds from Europe. The lack of significant trends in NO_3^- associated with
46 aerosols and precipitation under NEUS/SEUS flow is notable in light of the large decrease (37%)
47 in NO_x emissions in the US and Canada over the period of record. Rapid chemical processing of
48 oxidized N in marine air contributed to this lack of correspondence. Decreasing ratios of nss
49 SO_4^{2-} to NH_4^+ and the significant decreasing trend in precipitation acidity (37%) indicate that the
50 total amount of acidity in the multiphase gas-aerosol system in the western NAO troposphere
51 decreased over the period of record. Decreasing aerosol acidities would have shifted the phase
52 partitioning of total NH_3 ($\text{NH}_3 + \text{particulate } \text{NH}_4^+$) towards the gas phase thereby decreasing the
53 atmospheric lifetime of total NH_3 against wet plus dry deposition. The trend of increasing NH_4^+
54 in precipitation at Bermuda over the period of record suggests that NH_3 emissions from
55 surrounding continents also increased. Decreasing particulate nss SO_4^{2-} in near-surface air under
56 NEUS/SEUS flow over the period of record implies that the corresponding shortwave scattering
57 and absorption by nss S and associated aerosols constituents also decreased. These changes in
58 radiative transfer suggest a lower limit for net warming over the period in the range of 0.1 to 0.3
59 W m^{-2} .

60

61 1. Introduction

62

63 It has been recognized for many years that material emitted to the atmosphere from continental
64 sources can be transported long distances over adjacent oceans. For example, reports of crustal
65 aerosol transported from northern Africa over the open North Atlantic Ocean (NAO) have been
66 published in the scientific literature since the late 1700s (e.g., Dobson, 1781; Darwin, 1846).
67 More recently, trace elements and reaction products from S and N species emitted by
68 anthropogenic combustion and industrial sources were detected in atmospheric aerosols and
69 precipitation over the NAO (e.g., Zoller et al., 1973; Jickells et al., 1982; Chen and Duce, 1983).
70 Subsequent, studies have attempted to quantitatively differentiate relative contributions from
71 major source types (continental versus marine; anthropogenic versus biogenic versus crustal) and
72 major source regions based on analysis of elemental and molecular tracers (e.g., Arimoto et al.,
73 1995; Savioe et al., 2002), radionuclides (e.g., Arimoto et al., 1999), isotopic composition (e.g.,
74 Turekian et al., 2001, 2003; Hastings et al., 2003; Lin et al., 2012), air-mass transport history
75 (e.g., Moody and Galloway, 1988; Galloway et al., 1989; Moody et al., 1995, 2014), and satellite
76 remote sensing (e.g., Zhao et al., 2008; Zhang and Reid, 2010; Hsu et al., 2012; Prospero et al.,
77 2012). These and other studies indicate that the transport of anthropogenic emissions and
78 reaction products from North America is the dominant source of pollutants associated with
79 aerosols and precipitation over the western NAO at Bermuda. However, anthropogenic
80 emissions from surrounding continents have changed significantly over the past quarter century
81 suggesting that relative impacts of anthropogenic sources to air quality over the western NAO
82 have also changed.

83
84 Implementation of the Clean Air Act and associated amendments in the United States (US) and
85 similar legislation in Europe in the late 1980s and early 1990s led to substantial reductions in
86 emissions of SO₂ and NO_x to the atmosphere surrounding the North Atlantic basin (e.g.,
87 Vestreng, 2007; Hand et al., 2012). For example, emissions inventories prepared by the US
88 Environmental Protection Agency (EPA, 2013) indicate that, between 1980 and 2012, total
89 emissions of SO₂ and NO_x in the US decreased by factors of 80% and 50%, respectively. In
90 contrast, reported emissions of NH₃ in the US between 1990 (the earliest year available) and
91 2012 differed by less than 1% (EPA, 2013). Thus, the relative mixture of acids (from SO₂ and
92 NO_x oxidation) and bases in the planetary boundary layer (PBL) over the US and, presumably,
93 associated pH-dependent chemical processes, also evolved temporally over this period.
94 Reductions in SO₂ and NO_x emissions led to corresponding decreases in annual average SO₂ and
95 NO_x mixing ratios in ambient air over the US during the same period (factors of 78% and 56%,
96 respectively) (EPA, 2013). Concentrations of particulate-phase reaction products from the
97 oxidation of SO₂ and NO_x as well as aerosol optical depth (AOD) also decreased and visibility
98 improved. For example, between 2000 (the earliest year available) and 2012, average annual
99 concentrations of PM_{2.5} mass in near-surface air over the US decreased by 33% (EPA, 2013),
100 between 2000 and 2010, particulate SO₄²⁻ concentrations in rural areas of the US decreased by
101 27% (Hand et al., 2012), and, between 1980 and 2006, simulated AOD over the US decreased by
102 38% (Streets et al., 2009). Reductions in emissions have also led to large decreases in the
103 atmospheric deposition of SO₄²⁻, NO₃⁻ and H⁺ and the associated recovery of some degraded
104 watersheds in the eastern US (Kahl et al., 2004; Webb et al., 2004; Leibensperger et al., 2012).

105
106 The above trends for the US suggest that the physicochemical properties of the western NAO
107 atmosphere have also changed significantly over the past quarter century analogous to the sharp
108 decreases in lead over the NAO that followed phase out of leaded gasoline in the US (Shen and

109 Boyle, 1987). Although not significant, Zhang and Reid (2010) reported a decreasing trend in
110 AOD over the western NAO between 2000 and 2009. During the same period SO₂ and NO_x
111 emissions in the US decreased by 49% and 31%, respectively, and simulated AOD over the
112 continental US also decreased (Streets, et al., 2009). Based on satellite observations of AOD and
113 the chemical composition of near-surface aerosols, Moody et al (2014) estimate that, under
114 transport from the northeastern US during the period 2006 to 2009, pollutant aerosol accounted
115 for direct radiative cooling at Bermuda of 1.0 to 2.2 W m⁻². However, potential changes in AOD
116 resulting from emissions reductions in the US were not evaluated.

117

118 In this paper, we investigate long-term trends in the chemical composition of aerosols and
119 precipitation over the western NAO at Bermuda with a focus on evaluating impacts of emissions
120 reductions and influences of different source regions. This work is based on measurements
121 between 1989 and 1997 under the auspices of the Atmosphere Ocean Chemistry Experiment
122 (AEROCE) and comparable measurements between 2006 and 2009 at the same location.

123

124 2. Methods

125

126 2.1. Sampling Site, Periods, and Protocols

127

128 From June 1988 through July 1998, aerosols in sector (on-shore) flow at the Tudor Hill
129 Atmospheric Observatory (THAO) on Bermuda (32.27 N, 64.87 W) were sampled daily for
130 chemical characterization from the top of a 23-m scaffolding tower situated on a steep slope
131 about 25 m above sea level. Samples were collected in bulk at a nominal flow rate of 1.0 m³
132 min⁻¹ on Whatman 41 filters (20.3 x 25.4 cm) as part of AEROCE (Galloway et al., 1993; Savoie
133 et al., 2002). Data were blank corrected based on analysis of paired bulk-filter cassettes
134 deployed periodically in parallel with samples but through which no air was pulled.

135

136 From July 2006 through June 2009, dichotomous aerosol (nominal super- and sub- μ m-diameter
137 size fractions) was sampled daily at a rate of 0.1 m³ min⁻¹ with a custom-designed and fabricated
138 MSP model 130 high-flow cascade impactor configured with Liu-Pui type omnidirectional inlet
139 (Liu et al., 1983). Relative to MSP's Micro-Orifice Uniform Deposit Impactor (MOUDI)
140 (Marple et al., 1991) that is in more widespread use by the research community, these hi-flow
141 impactors yield greater signal per unit deployment time while segregating aerosol size fractions
142 using similar nozzle technology. Impactors were deployed at the top of the THAO tower
143 (Moody et al., 2014). The calculated inlet passing efficiency for 20- μ m-diameter particles was
144 95% and the 50% aerodynamic cut between the two size fractions was 0.8- μ m ambient diameter.
145 Impactors were configured with quartz-fiber (Pallflex 2500 QAT-UP) substrates (75-mm
146 diameter) and back filters (90-mm diameter). Dichotomous data were blank corrected based on
147 analysis of impactor substrates and back filters through which air was briefly pulled (~15 sec).
148 Between 2006 and 2009, a blank impactor was exposed and processed approximately once every
149 two weeks.

150

151 With the exception of the differences noted above, aerosol sampling and handling procedures
152 prior to analysis during both periods were virtually identical. Sampling was controlled by
153 sensors that activated pumps only during periods of no precipitation when surface winds were off
154 the ocean sector at speeds greater than 1 m sec⁻¹. Air volumes were measured with sharp-edged

155 flow tubes and normalized to standard temperature and pressure (0° C and 1 atm). Bulk cassettes
156 and impactors were cleaned with 18 MΩ cm⁻¹ deionized water (DIW), and dried, loaded, and
157 unloaded in a Class 100 clean bench mounted in a laboratory container at the base of the tower.
158 After recovery, exposed sample and blank filters and substrates were folded in half, sealed in
159 clean polyethylene bags, and stored (and shipped) frozen prior to analysis. Samples and
160 corresponding blanks during each period were processed and analyzed using identical analytical
161 procedures.

162
163 From July 1988 through April 1997 and from July 2006 through June 2009, wet-only
164 precipitation in unsectored air was sampled daily from the top of the THAO tower in precleaned
165 13.2 L polyethylene buckets mounted in an automated collector (Galloway et al., 1993).
166 Precipitation amount was measured in parallel with both bulk and recording rain gauges;
167 precipitation amounts reported herein correspond to those measured with the bulk gauge. After
168 recovery, sample aliquots (250 mL or less for low volume events) were transferred to precleaned
169 polyethylene bottles, sterilized on site via addition of 500 μL CHCl₃ to prevent microbial activity
170 (Keene et al., 1983; Herlihy et al., 1987), and stored refrigerated prior to analysis. During both
171 periods, precipitation was sampled and processed prior to chemical analysis using identical
172 procedures.

173 174 2.2. Sample Analysis

175
176 Aerosol sampled from 1988 to 1998 was analyzed at the University of Miami (UM) for SO₄²⁻,
177 NO₃⁻, and NH₄⁺ by suppressed ion chromatography (IC), and for Na⁺ by flame atomic absorption
178 spectroscopy (AA) (Galloway et al., 1993; Savoie et al., 2002). From 1988 to 1996, particulate
179 CH₃SO₃⁻ was also measured at UM by IC. Aerosols sampled from 2006 to 2009 were analyzed
180 at the University of Virginia (UVA) by IC for CH₃COO⁻, HCOO⁻, (COO)₂²⁻, CH₃SO₃⁻, SO₄²⁻, Cl⁻
181 , Br⁻, NO₃⁻, NH₄⁺, Na⁺, K⁺, Mg²⁺, and Ca²⁺ (Moody et al., 2014).

182
183 Precipitation sampled during both periods was analyzed for major ionic constituents at UVA.
184 From 1988 to 1997, H⁺ was measured by electrode and meter, anions (CH₃COO⁻, HCOO⁻,
185 CH₃SO₃⁻, SO₄²⁻, Cl⁻, Br⁻, and NO₃⁻) were measured by IC, NH₄⁺ was measured by the automated
186 indophenol blue technique, and base cations (Na⁺, K⁺, Mg²⁺, and Ca²⁺) were measured by AA
187 (Galloway et al., 1993). From 2006 to 2009, H⁺ was measured by electrode and meter and the
188 other major ions (the same suite as indicated above for aerosols during this period) were
189 measured by IC using procedures described by Moody et al. (2014).

190 191 2.3. Data Quality and Comparability

192
193 The quality of data for aerosols and precipitation sampled from 1988 to 1998 is described in
194 detail by Galloway et al. (1993) and Savoie et al. (2002). During both the earlier and later
195 sampling periods, data for aerosol samples that corresponded to in-sector times of less than 2.4
196 hours (10% of a day) exhibit low signal-to-noise and may not be representative; consequently,
197 these results were excluded from the final quality-assured data set. In addition, five samples
198 contained unusually high concentration of sea-salt constituents (30% to 380% higher than the
199 sample with the next highest concentrations) and/or operator notes that suggest direct

200 contamination by rainwater or splash; data for these samples were also excluded from the final
201 quality-assured data set.

202
203 Detection limits (DLs) for all analytes measured from 2006 to 2009 were estimated following
204 Keene et al. (1989). Because in-sector sampling times for aerosols included in the data set varied
205 from 10% to 100% of the corresponding deployment times, DLs for particulate-phase species
206 varied among samples and, thus, were calculated individually for each analyte in each sample
207 (Moody et al., 2014). Analytical performance was verified by intercomparison of the UVA
208 laboratory with those at UM and the University of New Hampshire, among others; routine
209 analysis of audit solutions from the National Institute of Standards and Technology, the World
210 Meteorological Association, and the US Environmental Protection Agency; periodic analysis of
211 standard additions to samples, and evaluation of ion balances and constituent ratios. These
212 comparisons indicate that the ionic data generated by both UVA and UM are unbiased.

213
214 Based on their thermodynamic properties (Henry's Law and dissociation constants), the
215 equilibrium phase partitioning of HNO_3 and NH_3 varies as a function of aerosol solution pH;
216 HNO_3 partitions preferentially with the less acidic super- μm size fractions of marine aerosol
217 whereas NH_3 partitions preferentially with the more acidic sub- μm size fractions (e.g., Moody et
218 al., 2014). In addition, larger aerosol size fractions in ambient air may be undersaturated with
219 respect to the gas phase because (1) their surface-to-volume ratios are relatively low and thus
220 equilibration times are relatively slow and (2) they exhibit relatively short atmospheric lifetimes
221 against deposition (e.g., Keene et al., 2004). When chemically distinct marine aerosols are
222 sampled in bulk (or in relatively coarse size fractions) the pH of the mixed sample may diverge
223 from those for the size fractions with which most NO_3^- and NH_4^+ was associated in ambient air
224 and thereby drive artifact phase changes (e.g., Keene et al., 1990). Explicit evaluation of the
225 magnitude of such artifacts is beyond the scope of this study but, because different sampling
226 methodologies were employed during the earlier and later periods, artifacts of this nature could
227 influence temporal trends based on measured particulate-phase concentrations of these analytes.
228 We return to this point below. Because H_2SO_4 is highly soluble over the reported range in
229 aerosol pH, particulate SO_4^{2-} is not subject to sampling artifacts of this nature.

230 231 2.4. Calculations

232
233 Contributions to measured SO_4^{2-} from sea-salt and non-sea-salt sources were differentiated
234 following (Keene et al., 1986) for all samples for which the measured concentrations of total
235 SO_4^{2-} and the sea-salt reference species were above detection limits (DL). Between 1988 and
236 1998, nss SO_4^{2-} associated with aerosols was calculated using Na^+ as the sea-salt reference
237 species and the mass ratio of SO_4^{2-} to Na^+ in surface seawater reported by Millero and Sohn
238 (1992) (0.2516). As indicated above, between 2006 and 2009, super- and sub- μm aerosol size
239 fractions were sampled on 75-mm and 90-mm diameter quartz-fiber substrates and filters,
240 respectively. Background concentrations of the two mostly commonly used sea-salt reference
241 species (Na^+ and Mg^{2+}) in extracts of blanks for the two filter sizes differed such that Na^+ offered
242 greater resolution in calculating nss SO_4^{2-} associated with the super- μm -diameter aerosol size
243 fraction whereas Mg^{2+} offered greater resolution for nss SO_4^{2-} associated with the sub- μm -
244 diameter size fraction. Super- and sub- μm -diameter nss SO_4^{2-} was calculated accordingly based
245 on the mass ratios of SO_4^{2-} to Na^+ and SO_4^{2-} to Mg^{2+} in surface seawater reported by Wilson

246 (1975), (0.2518 and 2.102, respectively). Minor differences between the seawater compositions
247 reported by Millero and Sohn (1992) and Wilson (1975) (less than 0.1%) used in the above
248 calculations were an insignificant source of bias in resulting nss concentrations. Over the entire
249 period of record, nss SO_4^{2-} in precipitation was calculated based on Na^+ as the reference species
250 and the seawater composition reported by Wilson (1975).

251
252 Concentrations of ionic species associated with super- and sub- μm -diameter aerosol size
253 fractions measured during 2006 to 2009 were summed (Moody et al., 2014) for comparison with
254 the chemical composition of aerosol sampled in bulk during the earlier period of record. To
255 evaluate temporal trends over the entire period of record, data were binned into sample years
256 based on the midpoint of the each daily sampling interval. Aerosol constituents are reported as
257 annual average concentrations and precipitation constituents are reported as VWA
258 concentrations. FLEXPART retroplumes (see below) were not available to characterize
259 transport for the samples collected prior to 1 January 1989. Consequently, from 1989 through
260 1997, sample years were defined as 1 January through 31 December and temporal trends were
261 interpreted based on the corresponding mid-year date of 1 July. Because the later 3-year period
262 of record started in mid-2006 and ended in mid-2009, sample years were defined as 1 July
263 through 30 June and interpreted based on the mid-year date of 1 January. This approach yielded
264 three full (12-month) sample years over the period of record. If based on calendar year, the last
265 six months of 2006 and the first six months of 2009 would have been excluded yielding only two
266 years for the analysis.

267 268 2.5. Atmospheric Transport

269
270 The particle dispersion model FLEXPART (Stohl et al., 1998, 2005) was run in backward mode
271 (Stohl et al., 2003; Seibert and Frank, 2004) to generate the column residence times and footprint
272 residence plots for source regions associated with the sampled air parcels. FLEXPART was
273 driven with ECMWF analyses of 0.36-degree resolution and accounts for turbulence and deep
274 convection in addition to the transport by grid-resolved winds. At 15 UTC (the approximate
275 midpoint of the deployment times for aerosol and precipitation samplers), 40,000 particles were
276 released from the location of the measurement site and followed backward in time for 10 days
277 Primary flow regimes were characterized based on proportional footprint residence times within
278 four prescribed source regions from which air was transported to Bermuda. See Moody et al.,
279 (2014) for detailed explanation of the procedure employed to identify primary air-mass source
280 regions for aerosols sampled at Bermuda during 2006 through 2009 and examples of retroplumes
281 for each flow regime. An identical approach was applied to characterize source regions for
282 aerosols sampled during 1989 to 1997 and for precipitation sampled during both periods. Wind
283 fields were not available for the first six months of 1990. Because retroplumes could not be
284 calculated for that period, annual statistics for 1990 were not included in the evaluation of trends
285 associated with air transported from different source regions.

286
287 Moody et al. (2014) identified two distinct flow regimes that transported aerosols from eastern
288 North America to Bermuda. One was associated with predominant flow from the northeastern
289 United States (NEUS) and southern Canada and the other with predominant flow from
290 southeastern US (SEUS) and the Gulf of Mexico. To evaluate trends associated with the
291 combined flow off northern and southern regions of eastern North America, the NEUS and

292 SEUS flow regimes were merged for this analysis into a single group (referred to as
293 'NEUS/SEUS'). Transport from northern Africa and the tropical NAO region (referred to as
294 'Africa') was associated with trade-wind flow along the southern portion of the Bermuda High
295 (BH). The 'Oceanic' flow regime was generally associated with long trajectories over the open
296 ocean under anticyclonic flow around the BH. The 'North' transport regime represented
297 transitional flow from the relatively clean open ocean to the polluted eastern North America.
298 Data evaluated herein were classified accordingly; the total numbers of samples and
299 corresponding mean precipitation amounts in the final data base partitioned by flow regime and
300 year are summarized in Table 1. The relatively fewer numbers of aerosol samples for the period
301 2006 to 2009 reflects the fact that 1) dichotomous rather than bulk aerosol was sampled during
302 the later period and thus the super- and sub- μm -diameter size fractions of each sample were
303 segregated and analyzed separately and 2) sampling rates through the high-flow impactor were a
304 factor of 10 lower than those through the hi-volume bulk sampler. Although analytical resolution
305 per unit analyte concentration in extract solutions was higher during the latter period, the
306 absolute amount of analyte present in each size fraction was lower relative to bulk aerosol during
307 the earlier part of the record. Consequently, relatively fewer aerosol constituents were present in
308 samples at concentrations above DLs during 2006 to 2009.

309

310 2.6. Statistical Evaluations

311

312 The statistical package SPSS was used to evaluate temporal trends in the data using two
313 complimentary approaches. (1) Trends were characterized based on slopes of standard linear
314 regressions (SLRs) for annual average concentrations of aerosol constituents versus time and for
315 annual VWA concentrations of precipitation constituents versus time. (2) Temporal trends in
316 annual mean (for aerosols) and annual VWA (for precipitation) constituent concentrations were
317 also characterized based on slopes calculated using the bootstrapping method applied to all
318 individual daily data (Freedman, 1981). The significance of each bootstrap slope was evaluated
319 using a two-tailed test based on 1000 random samples of the corresponding data subset. Relative
320 to SLRs, this method provides a more robust evaluation of significance in trends. For smaller
321 data sets, the approach resulted in redundant subsampling. In these cases the actual significance
322 thresholds may have deviated somewhat from the calculated values. However, sensitivity
323 evaluations employing smaller numbers of random samples yielded virtually identical results
324 suggesting that any such deviations were small to negligible. Interannual variability in mean or
325 VWA constituent concentrations is the only source of variance in the SLRs whereas seasonal
326 variability contributes significantly to overall variance based on the bootstrap method.
327 Consequently, substantially less overall variance in long-term trends is explained by
328 bootstrapping. Because this analysis focuses on long-term trends, reported variances correspond
329 to those for SLRs.

330

331 In addition to the calculations summarized above, trends in annual median aerosol and
332 precipitation concentrations and in per-event wet-deposition fluxes were also quantified for
333 selected data subsets to evaluate the sensitivity of results to the underlying sample statistics used
334 in the analysis. Results were reasonably consistent with those based on annual mean
335 concentrations for aerosols and annual VWA concentrations for precipitation. We interpret
336 results based on these latter more widely used conventions for reporting and evaluating

337 concentrations of aerosol and precipitation constituents thereby facilitating direct comparison
338 with previously published results.

339 3. Results and Discussion

341 3.1. Temporal Trends in the Chemical Composition of Aerosols and Precipitation

342 Temporal trends in annual average concentrations of particulate SO_4^{2-} , NO_3^- , and NH_4^+ and
343 corresponding trends in annual VWA concentrations in precipitation based on all quality-assured
344 data over the period of record at Bermuda are depicted in Figure 1. SO_4^{2-} concentrations for
345 both aerosols and precipitation decreased significantly but the percentage decrease in VWA
346 concentrations based on the SLR for precipitation (49%) was greater than the corresponding
347 decrease in annual mean concentrations for aerosols (24%, Table 2). In contrast, the VWA
348 concentration of NH_4^+ in precipitation increased significantly (70%) over the period of record
349 whereas the trend in particulate NH_4^+ was insignificant (Table 2). Concentrations of NO_3^-
350 associated with aerosols and precipitation also did not vary significantly (Table 2). These results
351 suggest long-term changes in atmospheric composition and also indicate that relative trends in
352 the composition of precipitation and near-surface aerosols diverge. However, substantial
353 interannual variability is evident for all species in both phases (Fig. 1a,b) and the corresponding
354 linear regressions explain less than 50% of the variance over the period of record.

355 3.2. Temporal Trends Based on FLEXPART Flow Patterns

356 Year-to-year variability in frequencies of transport from different source regions is one of the
357 major factors that drives interannual variability in atmospheric composition at a given location.
358 Such influences can be minimized by evaluating trends in concentrations as a function of
359 transport regime. As was the case for the data subset corresponding to aerosols sampled from
360 2006 to 2009 (Moody et al., 2014), segregation by source region differentiated analyte
361 concentrations into chemically distinct subgroups. For most years, the upper limits for mean
362 concentrations of aerosol and precipitation constituents were associated with polluted
363 NEUS/SEUS flow from North America whereas the lower limits were associated with
364 background Oceanic flow around the BH (Fig. 2). Analytes associated with the Africa and North
365 flow regimes generally fell within the range bounded by the other two regimes. However,
366 numbers of samples per year varied substantially among flow regimes (Table 1). The relatively
367 small numbers of samples collected under Oceanic and North flow in particular constrain the
368 power of statistical approaches for evaluating associated temporal trends and thus caution is
369 warranted in their interpretation.

370 Because regional transport varies seasonally, segregating data by source region also segregated
371 to some extent by season. For example, efficient transport of North American emissions over the
372 western NAO is typically associated with frontal passages, which are most frequent during
373 winter and spring, whereas transport from Northern Africa to the western NAO in association
374 with the easterly trade wind regime is most frequent during summer. Factors other than
375 precursor emissions within and the frequencies of flow from source regions also contribute to
376 seasonal variability in aerosol and precipitation composition among flow regimes. Relative to
377 colder months, higher ultraviolet radiation and temperatures during warmer months sustain faster

383 rates of precursor oxidation and secondary aerosol production. The temperature-dependent
384 emissions of NH₃ contribute to seasonal variability in the nucleation and growth of new particles.
385 Seasonal variability in precipitation fields and in the temperature-dependent partitioning of semi-
386 volatile species between the gas and particulate phases also drive seasonal variability in
387 atmospheric lifetimes and associated transport and deposition fields. Although these and other
388 processes contribute to overall variability in aerosol and precipitation composition as a function
389 of source region, our data lack adequate resolution to quantitatively differentiate relative
390 influences. See Moody et al. (2014) for a detailed evaluation of season variability in the sources
391 and composition of aerosols at Bermuda between 2006 and 2009.

392 393 3.1.1. nss SO₄²⁻

394
395 Based on slopes for SLRs fit to annual average concentrations, VWA nss SO₄²⁻ in precipitation
396 associated with the NEUS/SEUS flow regime decreased significantly (61%) over the period of
397 record whereas the corresponding trend in particulate nss SO₄²⁻ was marginally insignificant ($p =$
398 0.12 , Figs 2a,b, Table 2). The absence of a significant trend in particulate nss SO₄²⁻ for the
399 NEUS/SEUS flow was driven in part by the missing data for 1990. Based on all data (Fig. 1a),
400 1990 exhibited the highest mean concentration over the period and most samples during each
401 year were associated with the NEUS/SEUS regime (Table 1). Between 1989 and 2009, SO₂
402 emitted over the US and Canada decreased by 60% (Fig. 3). Although the overall decrease in
403 VWA nss SO₄²⁻ in precipitation based on the SLR was similar to that for SO₂ emissions over the
404 US and Canada during the period of record, the temporal patterns within the period of record
405 were distinct. Most of the decrease in VWA nss SO₄²⁻ was associated with a significant negative
406 trend between 1991 and 1996 (SLR slope = -0.62 , $r^2 = 0.84$, Fig. 2b). Based on the SLR for
407 1991 through 1996, annual VWA nss SO₄²⁻ during the period decreased by 51% whereas, over
408 the same period, SO₂ emissions in the US and Canada decreased by only 17% (Fig. 3). It is
409 evident from the above that (1) the declines in nss SO₄²⁻ associated with both near-surface
410 aerosols and precipitation under NEUS/SEUS flow were not directly proportional to the decline
411 in SO₂ emissions over the US and Canada and (2) factors other than SO₂ emissions over the
412 North American source region influenced trends in nss SO₄²⁻ associated with near-surface
413 aerosols and precipitation under NEUS/SEUS flow differentially.

414
415 Significant amounts of nss SO₄²⁻ associated with aerosols and precipitation at Bermuda originate
416 from the atmospheric oxidation of dimethylsulfide ((CH₃)₂S) produced in the surface ocean by
417 marine biota and subsequently emitted to the atmosphere (Galloway et al., 1989; Savoie et al.,
418 2002; Moody et al., 2014). Potential variability in biogenic contributions may have contributed
419 to the differences in trends noted above. To evaluate potential influences of biogenic S, we
420 employed the mass ratio of particulate nss SO₄²⁻ to CH₃SO₃⁻ yields from (CH₃)₂S oxidation
421 estimated from measurements at Bermuda (18.8 ± 2.2 , Savoie et al., 2002) to differentiate relative
422 contributions from marine biogenic and anthropogenic sources to annual average concentrations
423 of particulate nss SO₄²⁻ associated with NEUS/SEUS flow (Fig. 4a). Briefly, in mass units,
424 anthropogenic nss SO₄²⁻ was estimated from total nss SO₄²⁻ minus the product CH₃SO₃⁻ * 18.8.
425 Corresponding trends in annual VWA nss SO₄²⁻ in precipitation were calculated (Fig. 4b) based
426 on the assumption that the same product yields apply to precipitation. Trends in CH₃SO₃⁻ (and
427 thus biogenic contributions) for both aerosols and precipitation were insignificant, which
428 indicates that long-term temporal variability in nss SO₄²⁻ associated with both aerosols and

429 precipitation was driven primarily by differential variability in anthropogenic contributions.
430 These results also indicate that relative contributions of anthropogenic sources to VWA nss SO_4^{2-}
431 in precipitation at Bermuda have decreased more rapidly than those to mean nss SO_4^{2-} associated
432 with aerosols (Fig. 4). For example, based on the corresponding SLRs, percentage contributions
433 of anthropogenic sources to nss SO_4^{2-} in precipitation and aerosols under NEUS/SEUS flow were
434 roughly similar during the first sample year centered on 1 July 1989 (73% and 72%,
435 respectively) whereas they diverge to a greater degree by the final sample year centered on 1
436 January 2009 (41% and 68%, respectively). We return to this issue below.

437
438 VWA nss SO_4^{2-} associated with the Oceanic flow regime decreased significantly whereas the
439 corresponding trend in particulate nss SO_4^{2-} was insignificant (Fig. 2a,b, Table 2). Available
440 evidence suggests that virtually all particulate nss SO_4^{2-} in near-surface air sampled under
441 Oceanic flow at Bermuda between 2006 and 2009 originated from the oxidation of $(\text{CH}_3)_2\text{S}$
442 (Moody et al., 2014). Corresponding trends in CH_3SO_3^- associated with both aerosols and
443 precipitation sampled under Oceanic flow over the entire period of record were insignificant.
444 However, the relatively small numbers of observations per year (Table 1) coupled with seasonal
445 variability in CH_3SO_3^- concentrations (Moody et al., 2014) constrains resolution in explicitly
446 evaluating biogenic versus anthropogenic contributions to total nss SO_4^{2-} for this regime based on
447 product yields as was done for the NEUS/SEUS regime. However, the similarities in annual
448 mean particulate-phase nss SO_4^{2-} under Oceanic flow during both the earlier and later periods of
449 record (as reflected in the corresponding lack of a significant trend) indicates that the
450 background particulate nss SO_4^{2-} from biogenic sources in near-surface aerosol remained fairly
451 constant over this 20-year period. In contrast, VWA nss SO_4^{2-} in precipitation sampled under the
452 same flow regime exhibited significant decreasing concentrations. Most nss SO_4^{2-} in
453 precipitation originates from the aqueous-phase oxidation of SO_2 in cloud droplets and
454 scavenging of particulate nss SO_4^{2-} from the air column (e.g., Mari et al., 2000; von Glasow et
455 al., 2002) whereas aerosols evaluated herein were sampled near the surface. Our results suggest
456 the possibility that the transport of pollutant S emitted from surrounding continents sustained
457 relatively higher concentrations of oxidized S in aged marine air aloft, which contributed
458 significantly to nss SO_4^{2-} incorporated into precipitation but not into near-surface aerosols under
459 Oceanic flow. As anthropogenic emissions from surrounding continents decreased over the
460 period of record, contributions of pollutant S to background concentrations in aged marine air
461 aloft over the NAO would have also decreased thereby contributing to the observed decline
462 (61%) in VWA nss SO_4^{2-} in precipitation sampled under Oceanic flow (Fig. 2b, Table 2).

463
464 The larger decrease in VWA nss SO_4^{2-} associated with precipitation relative to aerosols in
465 NEUS/SEUS flow discussed above would be consistent with our interpretation of trends for the
466 Oceanic regime. Air masses transported off eastern North America over the western NAO may
467 rise up over and become decoupled from the marine boundary layer (MBL) (Neuman et al.,
468 2006) whereas most biogenic $(\text{CH}_3)_2\text{S}$ emitted from the ocean surface is oxidized within the
469 MBL (e.g., Savoie et al., 2002). Most SO_2 in the MBL is oxidized to particulate H_2SO_4 via
470 aqueous-phase pathways involving super- μm marine aerosols that have short lifetimes against
471 deposition and cloud droplets (e.g., Keene et al., 1998; von Glasow et al., 2002). In addition,
472 both SO_2 and sub- μm particulate nss SO_4^{2-} in the MBL are depleted via dry deposition to the
473 surface ocean. Consequently, oxidized S above the western NAO MBL, which available
474 evidence suggests is primarily anthropogenic, should exhibit longer atmospheric lifetimes

475 against removal relative to that within the MBL, which includes most of the biogenic component.
476 We hypothesize that the differential vertical distributions and associated atmospheric lifetimes of
477 oxidized S from anthropogenic versus biogenic sources coupled with reductions in
478 anthropogenic emissions contributed to relatively greater proportionate decreases in
479 anthropogenic contributions to nss SO_4^{2-} in precipitation versus near-surface aerosols over the
480 period of record. Corresponding trends in nss SO_4^{2-} associated with both aerosols and
481 precipitation sampled under North flow were insignificant (Fig. 2a,b, Table 2) but the relatively
482 small numbers of observations (Table 1) constrains resolution and, thus, caution is warranted in
483 interpreting these results.

484
485 Particulate nss SO_4^{2-} associated with the Africa flow regime decreased significantly (34%) over
486 the period of record (Fig. 2a, Table 2). Based on the SLR, corresponding VWA nss SO_4^{2-}
487 concentrations in precipitation under Africa flow generally decreased, but unlike aerosols, this
488 trend was not significant (Fig. 2b, Table 2). As was the case for the NEUS/SEUS regime, the
489 temporal trends in biogenic nss SO_4^{2-} (inferred from CH_3SO_3^- as described above) were
490 statistically indistinguishable from 0.0 for both aerosols (SLR slope = $-0.007 \text{ nmol m}^{-3} \text{ yr}^{-1}$) and
491 precipitation (SLR slope = $-0.006 \text{ } \mu\text{mol L}^{-1} \text{ yr}^{-1}$), which implies that reductions in anthropogenic
492 contributions drove the decreasing trends in nss SO_4^{2-} . We hypothesize that large reductions in
493 SO_2 emissions over Europe (Vestreng et al., 2007) coupled with transport over the subtropical
494 NAO in association with the easterly trade winds (e.g., Savoie et al., 1989) contributed to the
495 trend of decreasing particulate nss SO_4^{2-} for the Africa regime. However, unlike the differences
496 in trends under NEUS/SEUS flow discussed above, proportionate decreases in nss SO_4^{2-}
497 associated with aerosols and precipitation under Africa flow based on the SLR slopes (Fig. 2a,b)
498 were of roughly similar magnitude. Several factors may have contributed to differences in
499 temporal trends for aerosols versus precipitation based on available data for the two regimes.
500 Anthropogenic contributions to nss SO_4^{2-} under Africa flow were significantly less than those
501 under NEUS/SEUS flow (Moody et al., 2014). Based on the SLR for total particulate nss SO_4^{2-}
502 under Africa flow (Fig. 2a, Table 2) and that for the corresponding anthropogenic component
503 calculated as described above (not shown), anthropogenic contributions to particulate nss SO_4^{2-}
504 decreased from 46% to 19% between 1989 and 2008-09. Based on the SLRs, the corresponding
505 decrease for precipitation was of roughly similar magnitude (40% to 8%). Relative to the
506 NEUS/SEUS, the lower absolute contributions of anthropogenic S to an interannually variable
507 background of biogenic S afforded less resolution in evaluating trends for the Africa regime. In
508 addition, available observations under Africa flow were relatively less frequent (Table 1), which
509 further constrained resolution. Relatively longer transport times to Bermuda from Europe and
510 Africa versus North America as well as differences in associated atmospheric dynamics for the
511 two flow regimes may have also contributed to differences in trends. For example, during
512 transport over the ocean, losses of biogenic S via deposition to the surface are continually
513 replaced via oxidation of marine-derived $(\text{CH}_3)_2\text{S}$ whereas losses of anthropogenic S are not.
514 Consequently, vertical gradients in the relative abundance of oxidized S from anthropogenic
515 versus biogenic sources and the corresponding differences in ratios of anthropogenic to biogenic
516 S scavenged from the column by precipitation versus those for near-surface aerosols would be
517 expected to decrease with distance from anthropogenic source regions. Finally, to the extent
518 that interactions with mineral aerosol influence the atmospheric lifetime of oxidized S against
519 deposition, long-term temporal variability in mineral aerosol under transport from Africa to the

520 western NAO (e.g., Evan et al., 2006) may have modulated the trend in associated particulate nss
521 SO_4^{2-} relative to that for the NEUS/SEUS regime.

522 523 3.1.2. NO_3^-

524
525 Under NEUS/SEUS flow, trends based on SLRs fit to NO_3^- concentrations associated with both
526 aerosols and precipitation over the entire period of record were insignificant (Fig. 2c,d; Table 2).
527 In contrast, emissions of NO_x over the US and Canada decreased by 37% during this period (Fig.
528 3). The reported increase in NO_x emissions in the US between 2001 and 2002 reflects an artifact
529 that resulted from a change in the method used to estimate road emissions (R. L. Dennis, US
530 EPA, personnel communication, 2014). Like VWA nss SO_4^{2-} in precipitation at Bermuda, the
531 corresponding VWA NO_3^- also decreased significantly between 1991 and 1996 (SLR slope = -
532 0.50, $r^2 = 0.83$) but, unlike nss SO_4^{2-} , NO_3^- concentrations in precipitation recovered during the
533 latter period (2006 to 2009) to levels similar to those during the late 1980s and early 1990s (Fig.
534 2d). In contrast, NO_x emissions over the US and Canada decreased by only 1% between 1991
535 and 1996 (Fig. 3). Comparable decreases in particulate NO_3^- between 1991 and 1996 were not
536 evident (Fig. 2c). The annual average NO_3^- concentrations associated with aerosols under the
537 NEUS/SEUS regime were generally higher than those for other regimes whereas VWA
538 concentrations for precipitation overlapped to a greater degree (Fig. 2c,d). Presumably these
539 relatively higher concentrations reflect contributions from reaction products of pollutant NO_x
540 emitted over eastern North America. However, temporal trends in NO_3^- associated with both
541 near-surface aerosols and precipitation under NEUS/SEUS flow appear to be largely decoupled
542 from those of upwind NO_x emissions in the US. In addition, temporal variability in particulate
543 NO_3^- in near-surface aerosols was distinct from that for VWA NO_3^- in precipitation. We
544 speculate that the efficient oxidation of NO_x to HNO_3 in marine air coupled with the subsequent
545 partitioning of most HNO_3 with large, short-lived marine-aerosol (e.g., Russell et al., 2003;
546 Fischer et al., 2006; Keene et al., 2009) tended to attenuate temporal variability in near-surface
547 particulate NO_3^- under a given flow regime relative to both upwind emissions of precursor NO_x
548 and particulate species such as nss SO_4^{2-} and NH_4^+ that are associated primarily with longer-lived
549 sub- μm aerosol in marine air. The decreasing concentrations of primary marine aerosol with
550 altitude and corresponding influences on HNO_3 phase partitioning may have also contributed to
551 divergence in the temporal variability in near-surface particulate NO_3^- relative to NO_3^- scavenged
552 from the column by precipitation. However, corresponding trends in mean particulate Na^+ and
553 VWA Na^+ in precipitation at Bermuda (not shown) over the study period were not significant,
554 which implies that interannual variability in production of marine aerosol did not directly
555 influence trends in NO_3^- . It is unclear why temporal trends in HNO_3 and particulate NO_3^-
556 scavenged from the column by precipitation under NEUS/SEUS flow did not vary in response to
557 corresponding decreases in emissions of precursor NO_x over the upwind source region.

558
559 VWA NO_3^- in precipitation associated with flow from the North increased significantly over the
560 period of record (Fig. 2d, Table 2). All other trends in NO_3^- concentrations for both aerosols and
561 precipitation were insignificant at p of 0.05.

562 563 3.1.3. NH_4^+

564

565 Temporal trends in NH_4^+ associated with both aerosols and precipitation under NEUS/SEUS
566 flow were similar to those for NO_3^- ; none were significant (Fig. 2e,f and Table 2). The lack of
567 significant trends in NH_4^+ concentrations is consistent with expectations based on trends in
568 reported NH_3 emissions over the US and Canada, which increased by only 1% between 1990 and
569 2009 (Fig. 3). The reported decrease in NH_3 emissions in the US between 2000 and 2001 is an
570 artifact associated with a change in the method used to estimate emissions (R. L. Dennis, US
571 EPA, personnel communication, 2014). Like both nss SO_4^{2-} and NO_3^- , VWA NH_4^+
572 concentrations in precipitation decreased significantly during the early period of record (1991-
573 1996) (SLR slope = -0.19, $r^2 = 0.40$) and then recovered (Fig. 2f). In contrast, between 1991 and
574 1996, reported NH_3 emissions in the US and Canada increased by 9% (Fig. 3).

575
576 Like nss SO_4^{2-} , particulate NH_4^+ associated with the Africa regime decreased significantly over
577 the study period. In contrast, VWA NH_4^+ in precipitation sampled under Africa flow increased
578 significantly (Fig. 2e,f, Table 2). As discussed in more detail below, these opposite trends may
579 be driven in part by decreases in the acidity of the multiphase system and associate shifts in gas-
580 aerosol phase partition of NH_3 . All other trends in NH_4^+ were insignificant.

581 582 3.2. Implications

583
584 It is evident from the above that, in many cases, interannual variability and long-term trends in
585 mean nss SO_4^{2-} , NO_3^- , and NH_4^+ in near-surface aerosol associated with the major flow regimes
586 that transport air to Bermuda do not mirror corresponding patterns in VWA SO_4^{2-} , NO_3^- , and
587 NH_4^+ in precipitation (Fig. 2). Precipitation scavenges both soluble gases and particles from the
588 column whereas the measured aerosol composition reflects near-surface conditions. In addition,
589 relative to the column, near-surface air is chemically processed to a greater degree via
590 transformations involving freshly produced, large, and short-lived marine aerosol; direct
591 interactions with the ocean surface via the dry deposition of both precursor gases and particles;
592 and, emissions of $(\text{CH}_3)_2\text{S}$ and, under clean conditions, NH_3 (e.g., Bouwman et al., 1997) from
593 the ocean surface. These near-surface processes contribute to differential variability in the
594 composition of near-surface aerosols and precipitation reported herein. These results imply that,
595 relative to near-surface aerosols, the composition of precipitation may be a better indicator of
596 column-integrated trends in soluble atmospheric constituents. We also note that aerosol
597 sampling was sector controlled whereas precipitation sampling was not. However, available
598 evidence suggests that local emissions have minor to negligible influences on the composition of
599 wet-only precipitation at Bermuda (Galloway et al., 1988, 1989, 1993).

600
601 Trends in aerosol and precipitation composition associated with the NEUS/SEUS flow regime
602 did not track corresponding trends in emissions over the US and Canada during the entire study
603 period. Indeed, the significant and roughly similar proportionate decreases in VWA nss SO_4^{2-}
604 (factor of 2.2), NO_3^- (factor of 1.9), and NH_4^+ (factor of 1.8) in precipitation associated with
605 NEUS/SEUS flow between 1991 and 1996 (Figs. 2b, d, f) occurred in conjunction with
606 reductions in SO_2 and NO_x emissions over the US and Canada of only 17% and 1%, respectively,
607 and an increase on NH_3 emissions of 9% (Fig. 3). Corresponding patterns of decreasing
608 particulate phase concentrations were not evident (Figs 2a, c, e). These results imply that
609 physical processes such as trends in the efficiency of upwind removal via wet and dry deposition
610 as opposed to trends in upwind emissions drove the similar variability evident in the VWA

611 concentrations of these species during this period. In this regard, we note that variability in mean
612 precipitation amount per sample (Table 1) did not correlate with variability in VWA
613 precipitation composition, which indicates that dilution effects associated with storm size (e.g.,
614 Galloway et al., 1989) was not a major factor driving interannual variability or trends in
615 precipitation composition.

616
617 In contrast to the differences in concentrations associated with NEUS/SEUS flow and emissions
618 in the US and Canada evident in our data, between 1980 and 2010, wet-deposition fluxes of
619 SO_4^{2-} via precipitation and particulate SO_4^{2-} concentrations in near-surface air over the eastern
620 US decreased by 58% and 40%, respectively and the corresponding SO_2 emissions over the US
621 decreased by 56% (Leibensperger et al. 2012). Between 1980 and 2009, wet deposition fluxes of
622 NO_3^- over the eastern US decreased 33% while corresponding NO_x emissions decreased 36%.
623 Particulate NO_3^- concentrations over the eastern US were relatively uniform from 1990 to 2000
624 but decreased by 23% between 2000 and 2009 (Leibensperger et al. 2012). Wet deposition
625 fluxes of NH_4^+ over the eastern US during this period exhibited no significant trend whereas the
626 corresponding particulate NH_4^+ concentrations decrease by 30%. Comparisons with
627 measurements suggest that model calculations of these trends significantly underestimate the
628 decreases in particulate NO_3^- and NH_4^+ over this period (Leibensperger et al., 2012). Measured
629 and simulated trends over the downwind western NAO were not reported.

630
631 It is evident from the above that temporal variability in (1) spatial distributions of emission fields
632 over the NEUS/SEUS source region during the period of record, (2) the spatial distribution of
633 transport within the NEUS/SEUS flow regime, and/or (3) spatial distributions of deposition
634 fields under NEUS/SEUS flow contributed to temporal variability in aerosol and precipitation
635 composition at Bermuda. However, available information, and particularly the lack of spatially
636 resolved measurements of aerosol and precipitation composition over the western NAO
637 precludes quantitative evaluation of these factors. Our results highlight the difficulty in
638 characterizing influences of emissions reductions based on measurements at individual sites
639 located downwind.

640
641 Despite these limitations, results do provide unique insight regarding long-term trends in
642 regional atmospheric composition. For example, although only the trend in particulate NO_3^- was
643 marginally significant, all trends in NO_3^- and NH_4^+ associated with aerosols and precipitation
644 sampled under Oceanic flow over the period of record were positive and within a factor of about
645 2 in magnitude (31% to 67%. Fig. 2c,d,e, and f). The consistency of these patterns suggests that
646 background concentrations of inorganic N species in aged marine air within the NAO basin may
647 have increased over the past two decades. In contrast, the corresponding concentrations of VWA
648 nss SO_4^{2-} in precipitation associated with Oceanic flow decreased significantly (Fig. 2b, Table 2).

649
650 The changing mixture of acids and bases in the NAO troposphere impacts pH-dependent
651 chemical processes including the phase partitioning and associated atmospheric lifetimes against
652 deposition for compounds with pH-dependent solubilities. For example, trends of both aerosols
653 and precipitation based on all data (Fig. 1, Table 2) and the subset of data associated with
654 NEUS/SEUS flow (Fig. 2, Table 2) suggest that, on average, concentrations of nss SO_4^{2-}
655 decreased, NH_4^+ remained essentially unchanged or increased, and NO_3^- remained essentially
656 unchanged over the period of record. As discussed in Section 2.3, negative bias in particulate

657 NH_4^+ resulting from artifact volatilization of NH_3 from aerosol sampled in bulk during the early
658 part of the record may have contributed to the positive trend in particulate NH_4^+ but the positive
659 trend for precipitation is not subject to such artifacts. These data imply that, on average, acidities
660 of sub- μm -diameter aerosol solutions, with which most particulate nss SO_4^{2-} and NH_4^+ at
661 Bermuda was associated (Moody et al., 2014), decreased over the period, particularly during the
662 earlier part of the record. Decreasing aerosol acidities would have shifted the phase partitioning
663 of total NH_3 ($\text{NH}_3 + \text{NH}_4^+$) towards the gas phase (e.g., Smith et al., 2007) as is evident in the
664 changing molar ratios of nss SO_4^{2-} to NH_4^+ over the period (Fig. 5). For example, based on the
665 trend lines (Fig. 2, Table 2), between 1989 and 2009, ratios of mean nss SO_4^{2-} to NH_4^+ in near-
666 surface aerosols associated with NEUS/SEUS flow decreased from 1.2 to 1.1 (factor of 1.1)
667 whereas the corresponding ratios for VWA concentrations in precipitation decreased from 2.0 to
668 0.48 (factor of 4.3). The greater decrease in ratios for precipitation suggests that relative
669 contributions to NH_4^+ in precipitation from the scavenging of gaseous NH_3 versus particulate
670 NH_4^+ increased over the period. This increase in relative contributions from NH_3 would be
671 consistent with expectations based on a pH-dependent shift in the phase partitioning of total NH_3
672 towards the gas phase coupled with efficient scavenging of both NH_3 and particulate NH_4^+ by
673 precipitation. In addition, because dry deposition velocities to the ocean surface for NH_3 are
674 greater than those for sub- μm aerosol size fractions with which most NH_4^+ is associated in
675 ambient air (Smith et al., 2007; Moody et al., 2014), this shift would have resulted in an increase
676 in the average dry-deposition flux of total NH_3 to the ocean surface, a corresponding decrease in
677 the fraction of total NH_3 removed via wet deposition, and a decrease in the atmospheric lifetime
678 of total NH_3 against wet plus dry deposition. The long-term change in atmospheric acidity is
679 also evident in the significant decrease (37%) in VWA H^+ associated with precipitation sampled
680 under NEUS/SEUS flow over the period of record (SLR slope = -0.29, $r^2 = 0.49$, Fig. 6). We
681 recognize that trends reported herein are associated with large uncertainties, the corresponding
682 changes in phase partition and deposition are nonlinear, and explicit evaluation of trends in
683 aerosol solution pH and associated implications are not possible without paired measurements of
684 particulate and gas phase species. However, these relationships provide relevant quantitative
685 context for aspects of S and N cycling over the North Atlantic that are driven by changing
686 emissions over surrounding continents.

687
688 Despite the larger interannual variability evident in the temporal trends, our measurements and
689 associated interpretations suggest that concentrations and deposition fluxes of total NH_3 over the
690 western NAO increased during the period of record. However, EPA (2013) and Environment
691 Canada (2014) indicate that NH_3 emissions in the US and Canada did not vary significantly
692 between 1990 and 2009. If regionally representative, our results suggest the possibility that these
693 inventories may underestimate increasing trends in NH_3 emissions over North America.
694 Alternatively, increasing transport of NH_3 and particulate NH_4^+ from more distant sources in
695 Asia may have contributed to rising atmospheric concentrations over the NAO. In this regard,
696 Moody et al. (2014) detected significant mineral aerosol associated with NEUS flow that
697 available evidence suggests originated in Asia. Other studies have reported that the transport of
698 emission products from Asia significantly impact air quality over the western US although
699 corresponding impacts in the eastern US are relatively small to negligible (e.g., Koch et al.,
700 2007; Lin et al., 2014).

701

702 Because HNO₃ partitions primarily with less-acidic super- μm -diameter aerosols, its cycling in
703 marine air is largely decoupled from that of NH₃. In addition, most acidity added to larger
704 aerosol size fractions via accumulation of HNO₃ and H₂SO₄ is displaced to the gas phase in
705 association with HCl volatilization, which acts to regulate the pH of super- μm marine aerosols to
706 a fairly narrow range (low 3s to high 4s) over highly variable chemical regimes (e.g., Keene et
707 al., 2009). Consequently, relative to NH₃, HNO₃ cycling over the ocean is less sensitive to
708 changes in atmospheric acidity. Similarly, particulate NO₃⁻ is also less sensitive than NH₄⁺ to
709 artifact volatilization from marine aerosol sampled in bulk.

710
711 Our results also provide insight regarding the potential influence of reductions in SO₂ emissions
712 from North America on direct radiative forcing by pollutant aerosols over the western NAO at
713 Bermuda. Assuming that the marginally insignificant trend in particulate nss SO₄²⁻ associated
714 with NEUS/SEUS flow is reasonably representative of the actual long-term decline, the SLR
715 indicates that between 1989 and 2009, annual average concentrations for this flow regime
716 decreased by roughly 2.4 nmol m⁻³ or about 10% (Fig. 2a, Table 2). A regression fit to the
717 scatter plot of satellite AOD at 550 nm versus nss SO₄²⁻ associated with near-surface aerosol
718 under NEUS flow regime during 2006 to 2009 reported by Moody et al. (2014) yields a slope of
719 0.002 nmol⁻¹ m³. Assuming that trends in other aerosol constituents that scatter and/or absorb
720 radiation under this flow regime co-varied with particulate nss SO₄²⁻, the corresponding decrease
721 in AOD (0.005) coupled with satellite-derived estimates for the radiative efficiency of aerosols
722 per unit AOD in North American outflow over the ocean (-27 to -60 W m⁻² δ^{-1}) (Anderson et al.,
723 2005) yield an estimated net warming of 0.1 to 0.3 W m⁻² that resulted from the decreased
724 shortwave scattering and absorption by nss SO₄²⁻ and associated aerosol constituents under
725 NEUS/SEUS flow at Bermuda between 1989 and 2009. As discussed above, the greater
726 decreasing trend for nss SO₄²⁻ in precipitation relative to near-surface aerosols suggests that the
727 decline in particulate nss SO₄²⁻ in near surface air was less than that for oxidized S in the column
728 scavenged by precipitation. Consequently, this estimated range in warming should be considered
729 a lower limit. We appreciate that this approach is associated with large and poorly constrained
730 uncertainties but it is reasonably consistent with expectations based on model estimates of the
731 trend in net radiative warming of 0.8 W m⁻² over the US resulting from the reduction in
732 scattering and absorption by pollutant aerosols between 1990 and 2010 (Leibensperger et al.,
733 2012).

734 735 4.0. Summary

736
737 Since the 1980s, mandated reductions in SO₂ and NO_x emissions in the US, Canada, and Europe
738 have resulted in decreased export of oxidized S and N compounds to the NAO atmosphere.
739 Measurements at Bermuda between 1989 and 2009 indicate that nss SO₄²⁻ associated with
740 aerosols and precipitation decreased significantly (22% and 49%, respectively) whereas NH₄⁺
741 associated with precipitation increased significantly (70%) (Fig. 1, Table 2). Corresponding
742 trends in NO₃⁻ associated with aerosols and precipitation and of particulate NH₄⁺ were
743 insignificant.

744
745 To assess influences of emissions in upwind regions, data were stratified based on FLEXPART
746 retroplumes into four discrete transport regimes. Nss SO₄²⁻ in precipitation during NEUS/SEUS
747 and Oceanic flow decreased significantly (61% each) whereas corresponding trends in nss SO₄²⁻

748 associated with near-surface aerosols for both flow regimes were insignificant (Fig. 2a,b, Table
749 2). Available evidence supports the hypothesis that, for these flow regimes, ratios of
750 anthropogenic to biogenic contributions to nss SO_4^{2-} in the column scavenged by precipitation
751 were relatively greater than those for near-surface aerosol and, thus, precipitation provided a
752 better indicator of column-integrated trends.

753
754 Particulate nss SO_4^{2-} under African flow also decreased significantly (34%) whereas the
755 corresponding decrease in nss SO_4^{2-} associated with precipitation was insignificant (Fig. 2a,b,
756 Table 2). We infer that these trends were driven in part by reductions in the emissions and
757 transport of oxidized S compounds from Europe.

758
759 Insignificant trends in NO_3^- associated with aerosols and precipitation under NEUS/SEUS flow
760 (Fig. 2c,d, Table 2) did not reflect the large decrease in NO_x emissions in the US and Canada
761 over the period of record (Fig. 3). The rapid oxidation of NO_x in marine air coupled with
762 partitioning of most HNO_3 with large, short-lived marine aerosol may have attenuated trends in
763 NO_3^- concentrations relative to upwind NO_x emissions.

764
765 Trends of both aerosols and precipitation based on all data (Fig. 1) and the subset of data
766 associated with NEUS/SEUS flow (Fig. 2) suggest that, on average, concentrations of nss SO_4^{2-}
767 decreased, NH_4^+ remained essentially unchanged or increased, and NO_3^- remained essentially
768 unchanged, which implies that the total amount of acidity in the multiphase gas-aerosol system
769 in the western NAO troposphere decreased over the period of record. This interpretation is
770 consistent with the decreasing trend in VWA H^+ in precipitation under NEUS/SEUS flow
771 (Figure 6). The inferred decrease in aerosol acidities would have (1) shifted the phase
772 partitioning of total NH_3 towards the gas phase, (2) increased the dry deposition velocities for
773 total NH_3 to the ocean surface, (3) increased relative contributions to NH_4^+ in precipitation from
774 the scavenging of gaseous NH_3 versus particulate NH_4^+ , and (4) decreased the atmospheric
775 lifetime of total NH_3 against wet plus dry deposition.

776
777 Assuming that the marginally insignificant trend in particulate nss SO_4^{2-} in near-surface air
778 associated with NEUS/SEUS flow is reasonably representative of long-term temporal variability
779 (Fig. 2a, Table 2), decreasing concentrations over the period of record suggest a lower limit for
780 net warming in the range of 0.1 to 0.3 W m^{-2} resulting from decreased shortwave scattering and
781 absorption by nss SO_4^{2-} and associated aerosol constituents transported from North America over
782 the western NAO.

783
784 Acknowledgements

785
786 Dennis Savoie, Hal Maring, Kenneth Voss, and Miguel Izaguirre collaborated in conceptualizing
787 and conducting these research efforts. Annie Glasspool, Kim Zeeh and Chris Marsay assisted in
788 field operations and data generation and processing. Peter Sedwick and Andrew Peters
789 supervised operations at the THAO during the latter period of record and the Bermuda Institute
790 for Ocean Sciences provided outstanding logistical support during both measurement periods.
791 ECMWF provided meteorological data used to calculate FLEXPART retroplumes. Funding was
792 provided by the National Science Foundation through awards to the University of Virginia

793 (AGS-8701291, -9013128, -9414293, and -0541570) and the University of Miami (AGS-
794 8703411, -9013062, -9414262, and -0541566).

795 References

- 796
- 797 Anderson, T. L., Charlson, R. J., Bellouin, N., Boucher, O., Chin, M., Christopher, S. A.,
 798 Haywood, J., Kaufman, Y. J., Kinne, S., Ogren, J. A., Remer, L. A., Takemura, T., Tanré, D.,
 799 Torres, O., Trepte, C. R., Wielicki, B. A., Winker, D. M., and Yu, H.: An “A-Train” strategy
 800 for quantifying direct climate forcing by anthropogenic aerosols, *B. Am. Meteor. Soc.*, 12,
 801 1795-1809, 2005.
- 802 Arimoto, R., Duce, R. A., Ray, B. J., Ellis Jr., W. G., Cullen, J. D., and Merrill, J. T.: Trace
 803 elements in the atmosphere over the North Atlantic, *J. Geophys. Res.*, 100(D1), 1199-1213,
 804 1995.
- 805 Arimoto, R., Snow, J. A., Graustein, W. C., Moody, J. L., Ray, B. J., Duce, R. A., Turekian, K.
 806 K., and Maring, H. B.: Influences of atmospheric transport pathways on radionuclide
 807 activities in aerosol particles from over the North Atlantic, *J. Geophys. Res.*, 104(D17),
 808 21,301-21,316, 1999.
- 809 Bouwman, A. F., Lee, D. S., Asman, W. A. H., Dentener, F. J., Van Der Hock, K. W., and
 810 Olivier, J. G. J.: A global high-resolution emission inventory for ammonia, *Global*
 811 *Biogeochem. Cycles*, 11, 561-587, 1997.
- 812 Chen, L., and Duce, R. A.: The sources of sulfate, vanadium, and mineral matter in aerosol
 813 particles over Bermuda, *Atmos. Environ.*, 17, 2055-2064, 1983.
- 814 Darwin, C.: An account of this fine dust that often falls on vessels in the Atlantic Ocean,
 815 *Quarterly Journal of the Geological Society of London*, 2, 26-30, 1846.
- 816 Dobson, M.: An account of the Harmattan, a singular African wind, *Philosophical Transactions*
 817 *of the Royal Society of London*, 71, 46-57, 1781.
- 818 Environment Canada, Air Pollutant Emissions Data, [http://www.ec.gc.ca/inrp-npri/donnees-](http://www.ec.gc.ca/inrp-npri/donnees-data/ap/index.cfm?lang=En)
 819 [data/ap/index.cfm?lang=En](http://www.ec.gc.ca/inrp-npri/donnees-data/ap/index.cfm?lang=En) (last access: 22 May 2014), 2014.
- 820 EPA, National Emissions Inventory (NEI) Air Pollutant Emissions Trends Data, Office of Air
 821 Quality Planning and Standards, Technology Transfer Network, Clearing House for
 822 Inventories & Emissions Factors, <http://www.epa.gov/ttn/chief/trends/> (last access: 16
 823 [February 2014](http://www.epa.gov/ttn/chief/trends/)), 2013.
- 824 Evan, A. T., Heidinger, A. K., and Knippertz, P.: Analysis of winter dust activity off the coast of
 825 West Africa using a new 24-year over-water advanced very high resolution radiometer
 826 satellite dust climatology, *J. Geophys. Res.*, 111, D12210, doi:10.1029/2005JD006336, 2006.
- 827 Freedman, D. A.: Bootstrapping regression models, *Ann. Stat.*, 9, 1218-1228, 1981.
- 828 Fischer, E., Pszenny, A. Keene, W., Maben, J., Smith, A., Stohl, A., and Talbot, R.: Nitric acid
 829 phase partitioning and cycling in the New England coastal atmosphere, *J. Geophys. Res.*, 111,
 830 D23S09, doi:10.1029/2006JD007328, 2006.
- 831 Galloway, J. N., Tokos, Jr., J. J., Knap, A. H., and Keene, W. C.: Local influences on the
 832 composition of precipitation on Bermuda, *Tellus*, 40B, 178-188, 1988.
- 833 Galloway, J. N., Keene, W. C., Artz, R. S., Church, T. M., and Knap, S. H.: Processes
 834 controlling the concentrations of SO_4^- , NO_3^- , NH_4^+ , H^+ , HCOO_T and CH_3COO_T in
 835 precipitation on Bermuda, *Tellus*, 41B, 427-443, 1989.
- 836 Galloway, J. N., Savoie, D. L., Keene, W. C., and Prospero, J. M.: The temporal and spatial
 837 variability of scavenging ratios for nss sulfate, nitrate, methanesulfonate and sodium in the
 838 atmosphere over the North Atlantic Ocean, *Atmos. Environ.*, 27A, 235-250, 1993.

839 Hand, J. L., Schichtel, B. A., Malm, W. C., and Pitchford, M. L.: Particulate sulfate ion
840 concentration and SO₂ emission trends in the United States from the early 1990s through
841 2010, *Atmos. Chem. Phys.*, 12, 10,353–10,365, 2012.

842 Hastings, M. G., Sigman, D. M., and Lipschultz, F.: Isotopic evidence for source changes of
843 nitrate in rain at Bermuda, *J. Geophys. Res.*, 108(D24), 4790, doi:10.1029/2003JD003789,
844 2003.

845 Herlihy, L. J., Galloway, J. N., and Mills, A. L.: Bacterial utilization of formic and acetic acid in
846 rainwater, *Atmos. Environ.*, 21, 2397-2402, 1987.

847 Hsu, N. C., Gautam, R., Sayer, A. M., Bettenhausen, C., Li, C., Jeong, M. J., Tsay, S. C., and
848 Holben, B. N.: Global and regional trends of aerosol optical depth over land and ocean using
849 SeaWiFS measurements from 1997 to 2010, *Atmos. Chem. Phys.*, 12(17), 8037-8053,
850 doi:10.5194/acp-12-8037-2012. 2012

851 Jickells, T., Knap, A., Church, T., Galloway, J., and Miller, J.: Acid rain on Bermuda, *Nature*,
852 297, 55-57, 1982.

853 Kahl, J. S., Stoddard, J. L., Haeuber, R., Paulsen, S. G., Birnbaum, R., Deviney, F. A., Webb, J.
854 R., DeWalle, D. R., Sharpe, W., Driscoll, C. T., Herlihy, A. T., Kellogg, J. H., Murdoch, P.
855 S., Roy, K., Webster, K. E., and Urquhart, N. S.: Have U.S. surface waters responded to the
856 1990 Clean Air Act Amendments? *Environ. Sci. Technol.*, 38, 484A–490A, 2004.

857 Keene, W. C., Galloway, J. N., and Holden, Jr., J. D.: Measurement of weak organic acidity in
858 precipitation from remote areas of the world, *J. Geophys. Res.*, 88, 5122-5130, 1983.

859 Keene, W. C., Pszenny, A. A. P., Galloway, J. N., and Hawley, M. E.: Sea-salt corrections and
860 interpretation of constituent ratios in marine precipitation, *J. Geophys. Res.*, 91(D6),
861 6647-6658, 1986.

862 Keene, W. C., Talbot, R. W., Andreae, M. O., Beecher, K., Berresheim, H., Castro, M., Farmer,
863 J. C., Galloway, J. N., Hoffman, M. R., Li, S.-M., Maben, J. R., Munger, J. W., Norton, R. B.,
864 Pszenny, A. A. P., Puxbaum, H., Westberg, H., and Winiwarter, W.: An intercomparison of
865 measurement systems for vapor- and particulate-phase concentrations of formic and acetic
866 acids, *J. Geophys. Res.*, 94(D5), 6457-6471, 1989.

867 Keene, W. C., Pszenny, A. A. P., Jacob, D. J., Duce, R. A., Galloway, J. N., Schultz-Tokos, J. J.,
868 Sievering, H., and Boatman, J. F.: The geochemical cycling of reactive chlorine through the
869 marine troposphere, *Global Biogeochem. Cycles*, 4, 407-430, 1990.

870 Keene, W. C., Sander, R., Pszenny, A. A. P., Vogt, R., Crutzen, P. J., and Galloway, J. N.:
871 Aerosol pH in the marine boundary layer: A review and model evaluation, *J. Aerosol Sci.*, 29,
872 339-356, 1998.

873 Keene, W. C., Pszenny, A. A. P., Maben, J. R., Stevenson, E., and Wall A.: Closure evaluation
874 of size-resolved aerosol pH in the New England coastal atmosphere during summer, *J.*
875 *Geophys. Res.*, 109(D23), 307, doi:10.1029/2004JD004801, 2004.

876 Keene, W. C., Long, M. S., Pszenny, A. A. P., Sander, R., Maben, J. R., Wall, A. J., O'Halloran,
877 T. L., Kerkewg, A., Fischer, E. V., and Schrems, O.: Latitudinal variation in the multiphase
878 chemical processing of inorganic halogens and related species over the eastern North and
879 South Atlantic Oceans, *Atmos. Chem. Phys.*, 9, 7361-7385, 2009.

880 Koch, D., Bond, T. C., Streets, D., Unger, N., and van der Werf, R. G.: Global impacts of
881 aerosols from particular source regions and sectors, *J. Geophys. Res.*, 112(D2), D02205,
882 doi:10.1029,2005JD007024, 2007.

883 Leibensperger, E. M., Mickley, L. J., Jacob, D. J., Chen, W.-T., Seinfeld, J. H., Nenes, A.,
884 Adams, P. J., Streets, D. G., Kumar, N., and Rind R.: Climatic effects of 1950-2050 changes

885 in US anthropogenic aerosols - Part 1: Aerosol trends and radiative forcing, *Atmos. Chem.*
886 *Phys.*, 12, 3333-3348, doi:10.5194/acp-12-3333-2012, 2012.

887 Lin, C. T., A. R. Baker, T. D. Jickells, S. Kelly, and T. Lesworth, An assessment of the
888 significance of sulphate sources over the Atlantic Ocean based on sulphur isotope data,
889 *Atmos. Environ.*, 62, 615-621, 2012.

890 Lin, J., Pan, D., Davis, S. J., Zhang Q., He, K., Wang, C., Streets, D. G., Wuebbles, D. J., and
891 Guan, D.: China's international trade and air pollution in the United States, *P. Natl. Acad. Sci.*
892 *USA*, 21, 1-6, doi:10.1073/pnas.1312860111, 2014.

893 Liu, B. Y. H., Pui, D. Y. H., Wang, X. Q., and Lewis, C. W.: Sampling of carbon fiber aerosols,
894 *Aerosol Sci. Technol.*, 2, 499-511, 1983.

895 Mari, C., Jacob, D. J., and Bechtold, P.: Scavenging and transport of soluble gases in a deep
896 convective cloud, *J. Geophys. Res.*, 105(D17), 22,255-22,267, 2000.

897 Millero, F. J., and Sohn, M. L.: *Chemical Oceanography*, 531 pp., CRC Press, Boca Raton, Fl.,
898 1992.

899 Moody, J. L., and Galloway, J. N.: Quantifying the relationship between atmospheric transport
900 and the chemical composition of precipitation on Bermuda, *Tellus*, 40B, 463-479, 1988.

901 Moody, J. L., Oltmans, S. J., Levy II, H., and Merrill, J. T.: Transport climatology of
902 tropospheric ozone: Bermuda, 1988–1991, *J. Geophys. Res.*, 100(D4), 7179-7194, 1995.

903 Moody, J. L., Keene, W. C., Cooper, O. R., Voss, K. J., Aryal, R., Eckhardt, S., Holben, B.,
904 Maben, J. R., Izaguirre, M. A., and Galloway, J. N.: Flow climatology for physicochemical
905 properties of dichotomous aerosol over the western North Atlantic Ocean at Bermuda, *Atmos.*
906 *Chem. Phys.*, 14, 691-717, 2014.

907 Neuman, J. A., Parrish, D. D., Trainer, M., Ryerson, T. B., Holloway, J. S., Nowak, J. B.,
908 Swanson, A., Flocke, F., Roberts, J. M., Brown, S. S., Stark, H., Sommariva, R., Stohl, A.,
909 Peltier, R., Weber, R., Wollny, A., Sueper, D. T., Hubler G., and Fehsenfeld F. C.: Reactive
910 nitrogen transport and photochemistry in urban plumes over the North Atlantic Ocean. *J.*
911 *Geophys. Res.*, 111(D23), D23S54, doi: 10.1029/2005JD007010, 2006.

912 Prospero, J. M., Bullard, J. E., and Hodgkins, R.: High-latitude dust over the North Atlantic:
913 Inputs from Icelandic proglacial dust storms, *Science*, 335, 1078-1082, 2012.

914 Russell, K. M., Keene, W. C., Maben, J. R., Galloway, J. N., and Moody, J. L.: Phase-
915 partitioning and dry deposition of atmospheric nitrogen at the mid-Atlantic U.S. coast, *J.*
916 *Geophys. Res.*, 108(D21), 4656, doi:10.1029/2003JD003736, 2003.

917 Savoie, D. L., Prospero, J. M., and Saltzman, E. S.: Non-sea-salt sulfate and nitrate in tradewind
918 aerosols at Barbados: Evidence for long-range transport, *J. Geophys. Res.*, 94(D4), 5069-
919 5080, 1989.

920 Savoie, D. L., Arimoto, R., Keene, W. C., Prospero, J. M., Duce, R. A., and Galloway, J. N.:
921 Marine biogenic and anthropogenic contributions to non-sea-salt sulfate in the marine
922 boundary layer over the North Atlantic Ocean, *J. Geophys. Res.*, 107(D18), 4356,
923 doi:10.1029/2001JD000970, 2002.

924 Seibert, P. and Frank, A.: Source-receptor matrix calculation with a Lagrangian particle
925 dispersion model in backward mode, *Atmos. Chem. Phys.*, 4, 51-63, 2004.

926 Smith, A. M., Keene, W. C., Maben, J. R., Pszenny, A. a. P., Fischer, E., and Stohl, A.:
927 Ammonia sources, transport, transformation, and deposition in coastal New England during
928 summer, *J. Geophys. Res.*, 112, D10S08, doi:10.1029/2006JD007574, 2007.

929 Shen, G. T., and Boyle, E. A.: Lead in corals: Reconstruction of historical industrial fluxes to the
930 surface ocean, *Earth Planet Sci. Lett.*, 82, 289-304, 1987.

931 Stohl, A., Hittenberger, M., and Wotawa, G.: Validation of the Lagrangian particle dispersion
932 model FLEXPART against large scale tracer experiment data, *Atmos. Environ.*, 32, 4245-
933 4264, 1998.

934 Stohl, A., Forster, C., Eckhardt, S., Spichtinger, N., Huntrieser, H., Heland, J., Schlager, H.,
935 Wilhelm, S., Arnold, F., and Cooper, O.: A backward modeling study of intercontinental
936 pollution transport using aircraft measurements, *J. Geophys. Res.*, 108(D12), 4370,
937 doi:10.1029/2002JD002862, 2003.

938 Stohl, A., Forster, C., Frank, A., Seibert, P., and Wotawa, G.: Technical note: The Lagrangian
939 particle dispersion model FLEXPART version 6.2, *Atmos. Chem. Phys.*, 5, 2461-2474, 2005.

940 Streets, D. G., Yan, F., Chin, M., Diehl, T., Mahowald, N., Schultz, M., Wild, M., Wu, Y., and
941 Yu, C.: Anthropogenic and natural contributions to regional trends in aerosol optical depth,
942 1980–2006, *J. Geophys. Res.*, 114, D00D18, doi:10.1029/2008JD011624, 2009.

943 Turekian, V. C., Macko, S. A., and Keene, W. C.: Application of stable sulfur isotopes to
944 differentiate sources of size-resolved particulate sulfate in polluted marine air at Bermuda
945 during spring, *Geophys. Res. Lett.*, 28, 1491-1494, 2001.

946 Turekian, V. C., Macko, S. A., and Keene, W. C.: Concentrations, isotopic compositions, and
947 sources of size-resolved, particulate organic carbon and oxalate in near-surface marine air at
948 Bermuda during spring, *J. Geophys. Res.*, 108(D5), 4157, doi:10.1029/2002JD002053, 2003.

949 Vestreng, V., Myhre, G., Fagerli, H., Reis, S., and Tarrasón, L.: Twenty-five years of continuous
950 sulphur dioxide emission reduction in Europe, *Atmos. Chem. Phys.*, 7, 3663–3681, 2007.

951 von Glasow R., Sander, R., Bott, A., and Crutzen, P. J.: Modeling halogen chemistry in the
952 marine boundary layer. 2. Interactions with sulfur and cloud-covered MBL, *J. Geophys. Res.*,
953 107(D17), 4323, doi:10.1029/2001JD000943, 2002.

954 Webb, J. R., Cosby, B. J., Deviney, Jr., F. A., Galloway, J. N., Maben, S. W., and Bulger, A. J.;
955 Are brook trout streams in western Virginia and Shenandoah National Park recovering from
956 acidification? *Environ. Sci. Technol.*, 38, 4091–4096, 2004.

957 Wilson, T. R. S.: Salinity and the major elements of sea water, in *Chemical Oceanography*,
958 edited by J. P Riley and Skirrow, G. vol. 1, 2nd ed., pp. 365-413, Academic Press, Orlando,
959 FL, 1975.

960 Zhang, J., and Reid, J. S.: A decadal regional and global trend analysis of the aerosol optical
961 depth using a data-assimilation grade over-water MODIS and Level 2 MISR aerosol products,
962 *Atmos. Chem. Phys.*, 10, 10,949-10,0963, 2010.

963 Zhao, T. X. P., Laszlo, I., Guo, W., Heidinger, A., Cao, C., Jelenak, A., Tarpley, D., and
964 Sullivan, J.: Study of long-term trend in aerosol optical thickness observed from operational
965 AVHRR satellite instrument, *J. Geophys. Res.*, 113(D7), D07201.10.1029/2007JD009061,
966 2008.

967 Zoller, W. H., Gordon, G. E., Gladney, E. S., and Jones, A. G.: The sources and distribution of
968 vanadium in the atmosphere, in *Trace Elements in the Environment*, *Adv. Chem. Ser.*, vol.
969 123, 31-47, American Chemical Society, Washington, D.C., 1973.

970

971

972 Table 1. Numbers (Ns) of daily aerosol and precipitation samples and mean precipitation
 973 amounts (cm) per sample for all data evaluated in this study partitioned by flow regime and year.
 974 Annual data for 1989 through 1997 are binned by calendar year (1 January through 31
 975 December) and those for 2006 through 2009 are binned from 1 July through 30 June.
 976

<i>Mid Year</i>	1989	1990	1991	1992	1993	1994	1995	1996	1997	2007	2008	2009	All
<i>Aerosols, N</i>													
All Data ¹	168	184	199	186	130	152	174	182	215	113	111	84	1898
NEUS/SEUS	119	N/A	136	107	95	101	104	132	133	64	68	54	1113
Africa	30	N/A	41	45	24	28	40	32	49	26	30	22	367
Oceanic	9	N/A	11	17	3	11	9	8	10	6	8	5	97
North	10	N/A	11	17	8	12	21	10	23	17	5	3	137
<i>Precipitation, N</i>													
All Data ²	101	72	71	70	76	82	76	84	N/A	99	100	86	917
NEUS/SEUS	59	N/A	43	37	51	46	42	53	N/A	61	55	40	487
Africa	34	N/A	15	17	17	19	17	20	N/A	19	21	34	213
Oceanic	5	N/A	5	9	3	7	7	6	N/A	10	11	6	69
North	3	N/A	8	7	5	10	10	5	N/A	9	13	6	76
<i>Precipitation amount, cm</i>													
All Data	0.87	1.08	1.09	1.15	1.66	1.39	1.06	1.08	N/A	0.94	1.02	0.83	1.09
NEUS/SEUS	0.81	N/A	0.89	1.08	1.71	1.36	1.21	1.06	N/A	0.95	1.05	0.79	1.09
Africa	1.02	N/A	1.07	1.35	1.36	1.32	0.97	1.43	N/A	1.07	1.02	0.77	1.10
Oceanic	0.90	N/A	0.56	1.28	1.00	1.93	1.06	0.51	N/A	1.11	0.76	0.99	1.03
North	0.35	N/A	2.53	0.90	2.49	1.31	0.60	0.57	N/A	0.36	1.14	1.31	1.16

977
 978 N/A indicates that either the chemical data or the corresponding FLEXPART retroplumes were
 979 not available for the indicated period (see text).

980
 981 ¹Ns correspond to particulate nss SO₄²⁻, NO₃⁻, and NH₄⁺; for particulate CH₃SO₃⁻, total N was
 982 1266 due to the shorter period of record and relatively fewer samples with concentrations greater
 983 than DLs.

984
 985 ²Ns corresponds to nss SO₄²⁻, NO₃⁻, and NH₄⁺ in precipitation; for CH₃SO₃⁻ in precipitation, total
 986 N was 845 due to the relatively fewer samples with concentrations greater than DLs.

987 Table 2. Regression statistics and, for significant trends, percent changes in concentrations over
 988 the period of record.

Species / Flow Regime	Bootstrap Slope (Std.Error) (nmol m ⁻³ yr ⁻¹)	SLR Slope(nmol m ⁻³ yr ⁻¹)	SLR r ²	SLR Change ¹ (%)	Bootstrap Slope (Std. Error) (μmol L ⁻¹ yr ⁻¹)	SLR Slope (μmol L ⁻¹ yr ⁻¹)	SLR r ²	SLR Change ¹ (%)
	Aerosol				Precipitation			
<i>nss SO₄²⁻</i>								
All Data	-0.26(0.08)*	-0.24	0.17	-22%	-0.10(0.03)*	-0.11	0.67	-49%
NEUS/SEUS	-0.16(0.11)	-0.12	-	-	-0.16(0.05)*	-0.17	0.61	-61%
Africa	-0.28(0.12)*	-0.31	0.29	-34%	-0.06(0.06)	-0.06	-	-
Oceanic	0.14(0.12)	0.14	-	-	-0.09(0.03)*	-0.08	0.31	-61%
North	0.36(0.34)	0.22	-	-	0.10(0.06)	0.04	-	-
<i>NO₃⁻</i>								
All Data	-0.01(0.05)	-0.01	-	-	0.05(0.03)	0.04	-	-
NEUS/SEUS	0.03(0.07)	0.03	-	-	0.02(0.05)	0.01	-	-
Africa	-0.12(0.06)**	-0.13	0.26	-20%	0.08(0.05)	0.07	-	-
Oceanic	0.17(. 09)**	0.18	0.53	46%	0.06(0.05)	0.06	-	-
North	0.23(0.17)	0.31	-	-	0.17(0.06)*	0.13	0.32	76%
<i>NH₄⁺</i>								
All Data	-0.05(0.08)	-0.06	-	-	0.08(0.03)*	0.08	0.68	70%
NEUS/SEUS	0.05(0.10)	0.04	-	-	0.08(0.05)	0.09	-	-
Africa	-0.33(0.11)*	-0.33	0.35	-44%	0.09(0.05)**	0.09	0.48	102%
Oceanic	0.05(0.16)	0.09	-	-	0.03(0.03)	0.03	-	-
North	0.15(0.26)	0.05	-	-	0.09(0.06)	0.05	-	-

989

990 * $p = 0.05$; significant at 95% confidence.

991 ** $p = 0.10$; significant at 90% confidence.

992 ¹Percent change over the period of record relative to 1989 based on the SLR slope.

993

994 Figure Caption

995

996 Figure 1. Temporal trends in (a) annual average concentrations of bulk particulate nss SO_4^{2-}
997 (red), NO_3^- (blue), and NH_4^+ (green) in near-surface air (white backgrounds) and (b)
998 corresponding annual VWA concentrations in precipitation (light blue backgrounds) at
999 Bermuda based on all quality-assured data generated over the period of record. Color-coded
1000 dashed lines correspond to SLRs for annual averages and VWAs versus time.

1001

1002 Figure 2. Temporal trends in annual average concentrations of bulk particulate (a) nss SO_4^{2-} , (c)
1003 NO_3^- , and (e) NH_4^+ in near-surface air (white backgrounds) and annual VWA concentrations
1004 of (b) nss SO_4^{2-} , (d) NO_3^- , and (f) NH_4^+ in precipitation (light blue backgrounds) associated
1005 with NEUS/SEUS (red), African (yellow), Oceanic (blue), and North (green) flow regimes.
1006 Color-coded dashed lines correspond to SLRs for annual mean and VWA concentrations
1007 versus time.

1008

1009 Figure 3. Temporal trends in SO_2 (red), NO_x (blue), and NH_3 (green) emitted to the atmosphere
1010 over the continental US (EPA, 2013) and over the continental US plus Canada (Environment
1011 Canada, 2014; solid line) during the period of this study.

1012

1013 Figure 4. Temporal trends in anthropogenic and biogenic contributions to nss SO_4^{2-} associated
1014 with (a) aerosols (white backgrounds) and (b) precipitation (light blue backgrounds) sampled
1015 under NEUS/SEUS flow.

1016

1017 Figure 5. Temporal trends in (a) ratios of annual mean concentrations of particulate nss SO_4^{2-}
1018 versus NH_4^+ (white backgrounds) and (b) corresponding ratios of annual VWA concentrations
1019 in precipitation (light blue backgrounds) associated with NEUS/SEUS (red), African (yellow),
1020 Oceanic (blue), and North (green) flow regimes and for all data (black).

1021

1022 Figure 6. Temporal trend in annual VWA H^+ in precipitation associated with NEUS/SEUS flow.

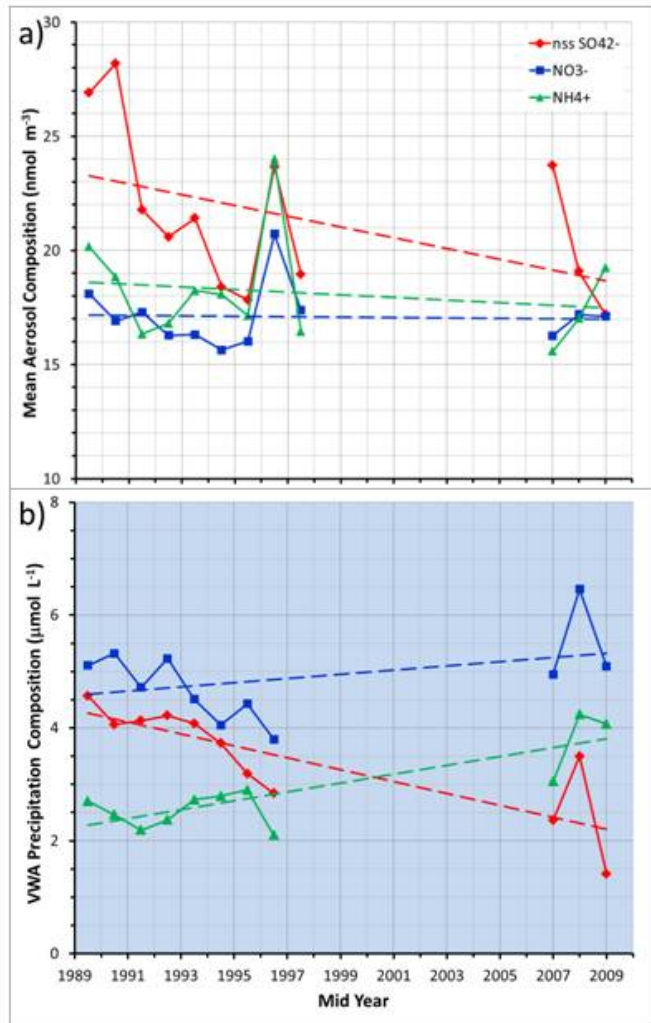


Figure 1

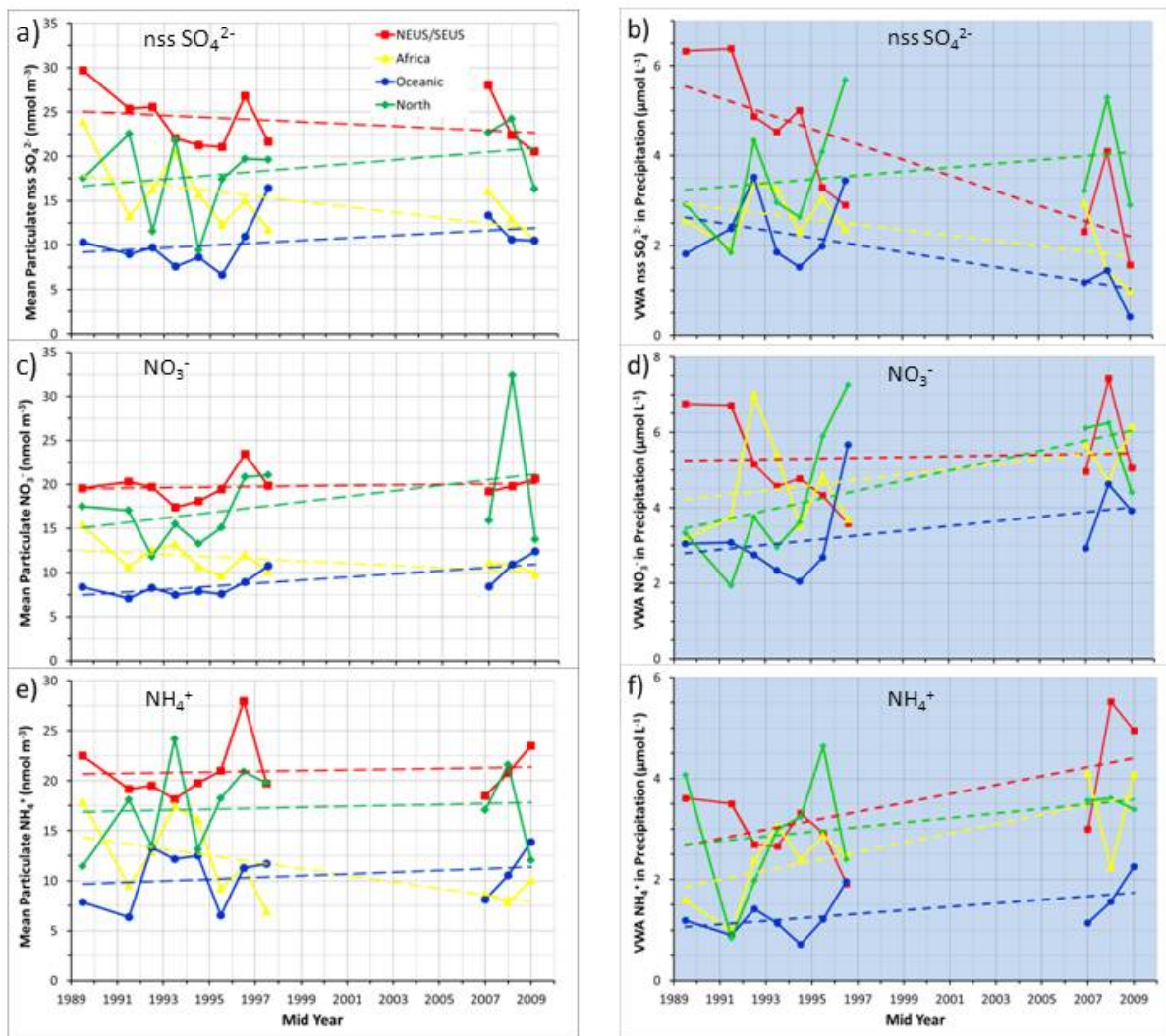


Figure 2

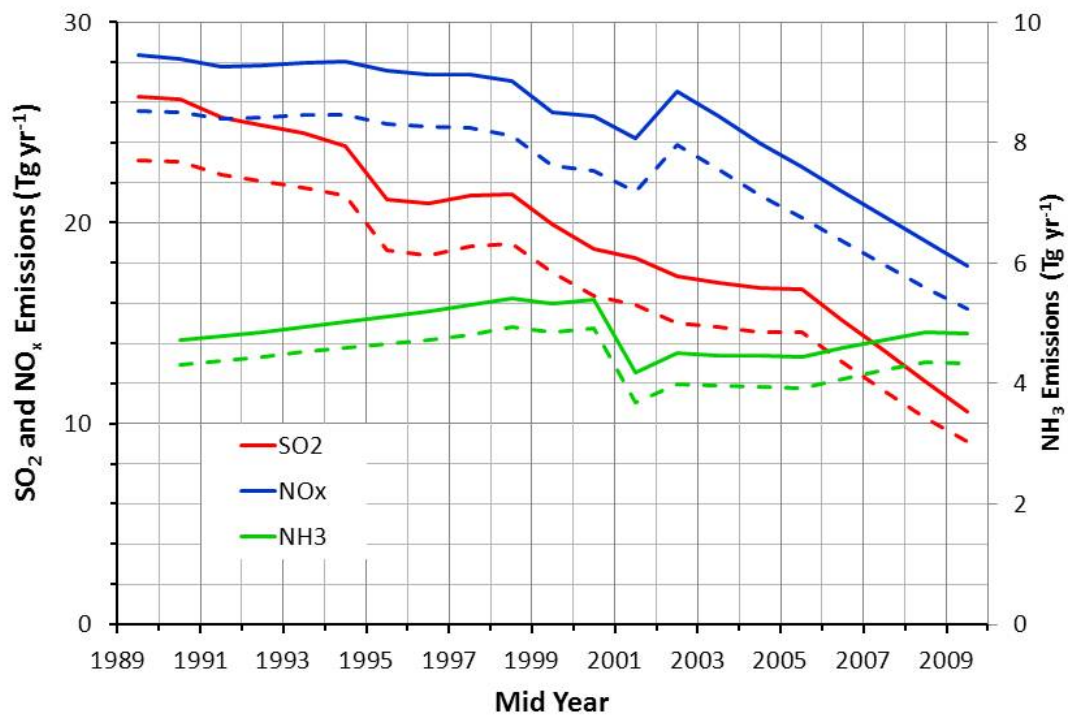


Figure 3

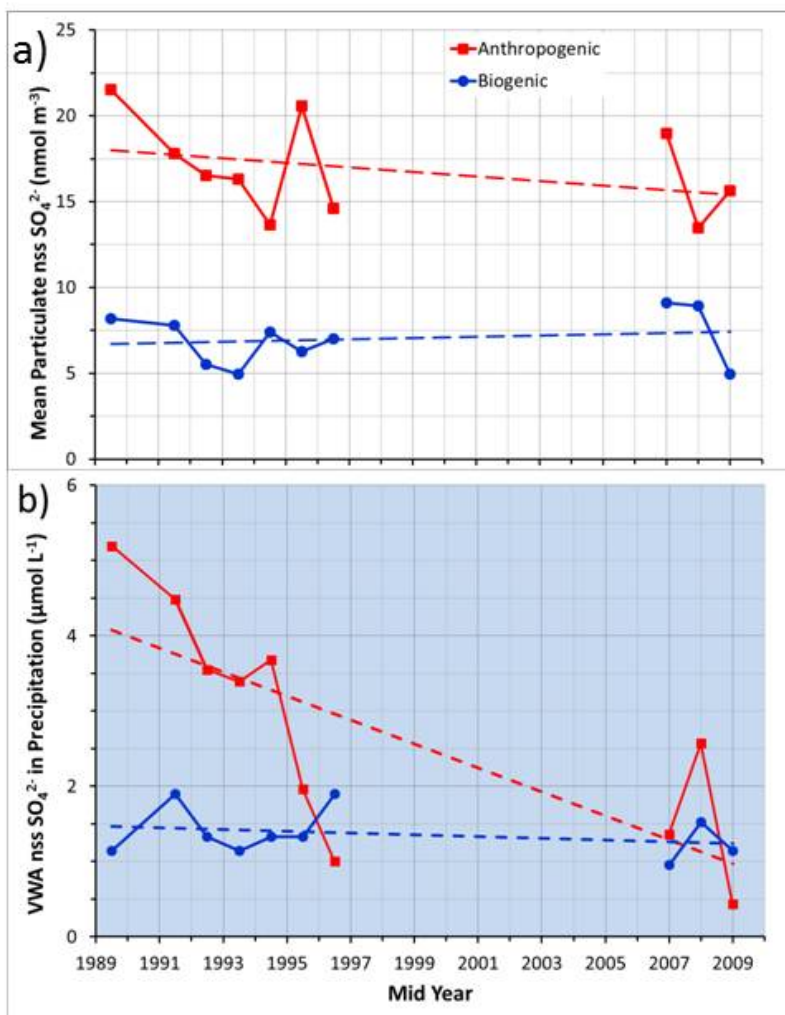


Figure 4

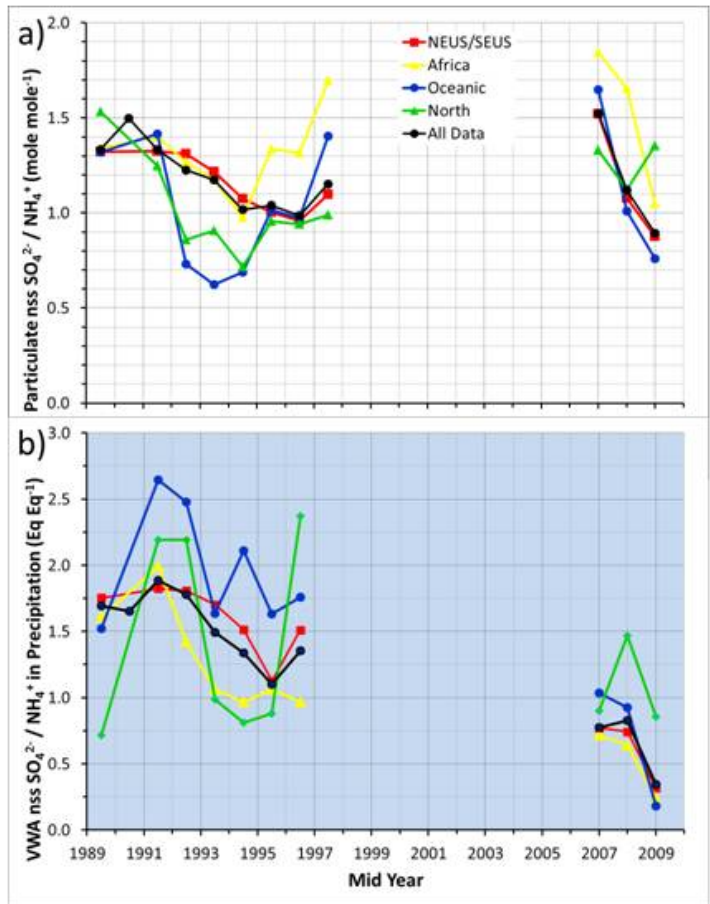


Figure 5

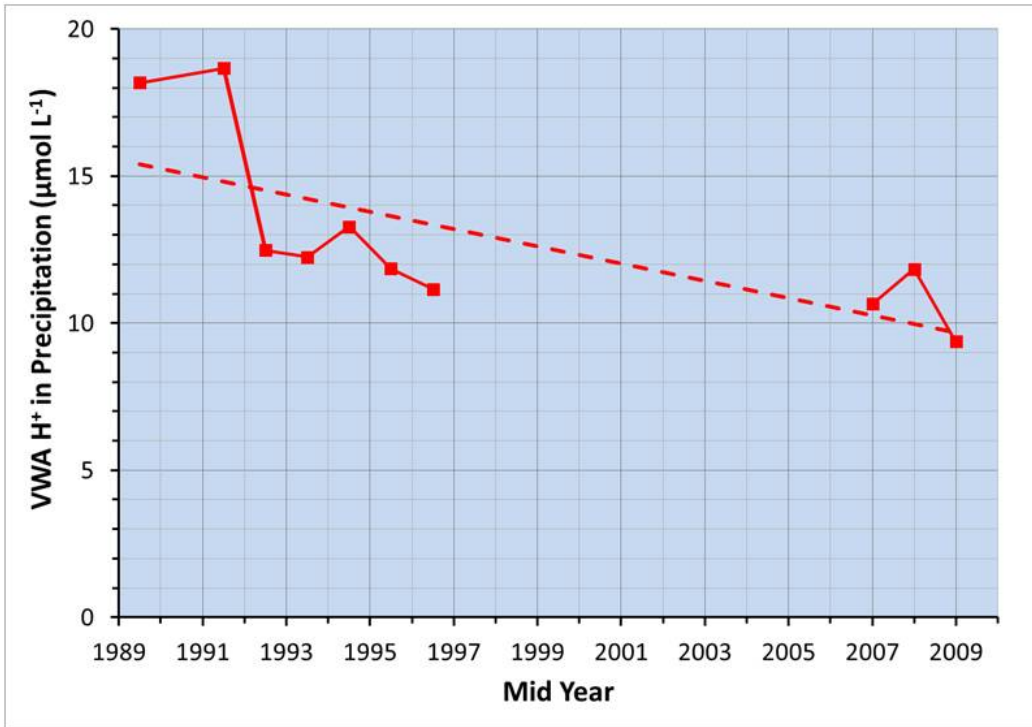


Figure 6